



Synthesis and luminescent properties of novel red-emitting $M_7Sn(PO_4)_6:Eu^{3+}$ ($M = Sr, Ba$) phosphors

Guo Feng^{1,*}, Weihui Jiang^{1,2,3,*}, Jianmin Liu¹, Cong Li¹, Quan Zhang¹

¹National Engineering Research Center for Domestic & Building Ceramics, Jingdezhen Ceramic Institute, Jingdezhen 333000, China

²Department of Material Science and Engineering, Jingdezhen Ceramic Institute, Jingdezhen 333000, China

³Jiangxi Key Laboratory of Advanced Materials, Jingdezhen 333000, China

Received 17 March 2017; Received in revised form 6 October 2017; Received in revised form 20 November 2017;

Accepted 18 January 2018

Abstract

Novel Eu^{3+} -activated $M_7Sn(PO_4)_6$ (where $M = Sr, Ba$) red-emitting phosphors were synthesized via conventional solid-state reaction method at 1200 °C for 2 h. The luminescence properties of the prepared samples and quenching concentration of $Sr_{7-x}Sn(PO_4)_6:xEu^{3+}$ and $Ba_{7-x}Sn(PO_4)_6:xEu^{3+}$ were investigated. These phosphors can be efficiently excited by UV (395 nm) and visible blue (465 nm) light nicely matching the output wavelengths of the near-UV LEDs and InGaN blue LED chips and emit the red light. The critical concentrations of the Eu^{3+} activator were found to be 0.175 mol and 0.21 mol per formula unit for $Sr_{7-x}Sn(PO_4)_6:xEu^{3+}$ and $Ba_{7-x}Sn(PO_4)_6:xEu^{3+}$, respectively. The $M_{7-x}Sn(PO_4)_6:xEu^{3+}$ ($M = Sr, Ba$) phosphor may be a good candidate for light-emitting diodes application.

Keywords: strontium tin phosphate, barium tin phosphate, Eu^{3+} -doping, red phosphors, luminescence

I. Introduction

Solid state lighting based on InGaN light-emitting diodes (LED) shows significant potential for replacing conventional lighting sources, such as incandescent and fluorescent lamps, because of their high luminous efficiency, energy-saving, long lifetime and environmental protection. In this field, there are three different methods that can be used to realize white light emitting: i) red-green-blue (RGB) light emitting diode chips combined directly, ii) blue-LED chip combined with yellow (or green and red) wavelength conversion phosphor and iii) near-ultraviolet LED chip combined with RGB wavelength conversion phosphor [1–5].

Inorganic phosphors typically consist of an inert host lattice that is doped with activator ions, usually transition (3d) or rare-earth (4f) metals. The host lattice is transparent for the incident radiation and the activator is excited to emit photons [6]. In recent years, extensive

research has been carried out on rare-earth-doped phosphors because of several important superior properties, such as luminescent characteristics, stability in vacuum, and corrosion-free gas emission under electron bombardment compared with traditional cathode ray tube used in current field emission displays [7,8]. Trivalent Eu ion, as one of the promising species that provide optical emission in red colour regions, has been doped in various compounds [9–11]. However, to the best of our knowledge, there is no report on the research of $M_7Sn(PO_4)_6$ ($M = Sr, Ba$) phosphor activated by rare earth or transition metal.

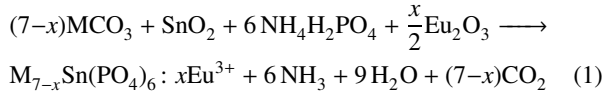
In this work, new luminescent material $M_7Sn(PO_4)_6:Eu^{3+}$ ($M = Sr, Ba$) was synthesized, its luminescence properties and the Eu^{3+} concentration dependence of the emission properties were investigated.

II. Experimental

Strontium carbonate $SrCO_3$ (A.R.), barium carbonate $BaCO_3$ (A.R.), tin dioxide SnO_2 (A.R.), ammo-

*Corresponding author: tel: +86 798 8499000,
e-mail: fengguo@jci.edu.cn (Guo Feng)
whj@jci.edu.cn (Weihui Jiang)

niium dihydrogen phosphate $\text{NH}_4\text{H}_2\text{PO}_4$ (A.R.), and europium oxide Eu_2O_3 (A.R.) were taken as starting materials. Stoichiometric amounts of these materials were weighted as the nominal composition of $\text{M}_{7-x}\text{Sn}(\text{PO}_4)_6 : x\text{Eu}^{3+}$ (where $\text{M} = \text{Sr}, \text{Ba}$ and $x = 0, 0.035, 0.07, 0.105, 0.14, 0.175, 0.21, 0.245$). Then they are blended and mixed in agate mortar. The finely ground powders were directly placed in a high dense Al_2O_3 crucible and processed by conventional solid state reactions route at 1200°C for 2 h at ambient air atmosphere. Following reactions occurred, where $\text{M} = \text{Sr}$ or Ba :

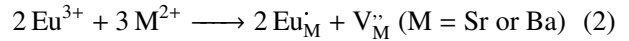


The structure of $\text{M}_7\text{Sn}(\text{PO}_4)_6 : \text{Eu}^{3+}$ phosphors was identified by recording the powder X-ray diffraction (XRD) patterns using X'pert PRO X-ray diffractometer with $\text{CuK}\alpha_1$ radiation ($\lambda = 1.54056 \text{ \AA}$). Scanning electron microscope (SEM, PHENOM Pr) was employed to analyse the morphology and microstructure of the typical $\text{Sr}_{6.86}\text{Sn}(\text{PO}_4)_6 : 0.14\text{Eu}^{3+}$ and $\text{Ba}_{6.86}\text{Sn}(\text{PO}_4)_6 : 0.14\text{Eu}^{3+}$ phosphors. Excitation and emission spectra were measured at room temperature by using Hitachi F-4500 spectrofluorometer equipped with a 60 W Xenon lamp as excitation source.

III. Results and discussion

Figure 1 shows the typical XRD patterns of the $\text{M}_{7-x}\text{Sn}(\text{PO}_4)_6 : x\text{Eu}^{3+}$ samples, where $\text{M} = \text{Sr}$ or Ba and $x = 0$ or 0.14 . The XRD patterns of the samples $\text{Sr}_7\text{Sn}(\text{PO}_4)_6$ and $\text{Sr}_{6.86}\text{Sn}(\text{PO}_4)_6 : 0.14\text{Eu}^{3+}$ matched well with JCPDS 33-1355 card (corresponding to cubic $\text{Sr}_7\text{Sn}(\text{PO}_4)_6$), and the XRD patterns of the samples $\text{Ba}_7\text{Sn}(\text{PO}_4)_6$ and $\text{Ba}_{6.86}\text{Sn}(\text{PO}_4)_6 : 0.14\text{Eu}^{3+}$ agreed well with JCPDF 34-0064 card (correspond-

ing to cubic $\text{Ba}_7\text{Sn}(\text{PO}_4)_6$). In all the samples no characteristic peaks of the raw materials or other impurities were detected. The diffraction peak positions and relative intensities of the samples $\text{Sr}_7\text{Sn}(\text{PO}_4)_6$ and $\text{Ba}_7\text{Sn}(\text{PO}_4)_6$ are consistent with the JCPDS values. In contrast, a slight diffraction angle shift to higher angles are observed in the diffraction patterns of the doped samples ($\text{Sr}_{6.86}\text{Sn}(\text{PO}_4)_6 : 0.14\text{Eu}^{3+}$ and $\text{Ba}_{6.86}\text{Sn}(\text{PO}_4)_6 : 0.14\text{Eu}^{3+}$) suggesting a decrease in the interplanar distance, which is due to the two main reasons: i) the substitution of Sr^{2+} (the ionic radius of 0.127 nm) and Ba^{2+} (the ionic radius of 0.143 nm) by Eu^{3+} with smaller ionic radius (0.113 nm) and ii) vacancy in structure introduced by unequal valence substitution according to equation (2). In addition, the XRD patterns also indicate that Eu^{3+} does not significantly influence the structure of the host, and the single-phased phosphors can be obtained successfully in our experimental conditions.



SEM analyses were employed to investigate the morphology and particle size of the samples $\text{Sr}_{6.86}\text{Sn}(\text{PO}_4)_6 : 0.14\text{Eu}^{3+}$ and $\text{Ba}_{6.86}\text{Sn}(\text{PO}_4)_6 : 0.14\text{Eu}^{3+}$. The typical morphological images, represented in Fig. 2, show that both of these phosphors have regularly shaped individual particles with clearcut edges, which indicates excellent crystallinity of phosphors. The surface of the powders has many pores and voids. They may be formed by volatile gases exiting matrix (CO_2 and NH_3 , equation (1)). The micrograph referring to the obtained phosphors shows the presence of large agglomerates in the irregular rigid block form of approximately $10 \mu\text{m}$. The average grain size is on micrometric scale.

The fluorescence excitation spectra of the samples $\text{Sr}_{6.86}\text{Sn}(\text{PO}_4)_6 : 0.14\text{Eu}^{3+}$ and $\text{Ba}_{6.86}\text{Sn}(\text{PO}_4)_6 : 0.14\text{Eu}^{3+}$ were shown in Fig. 3.

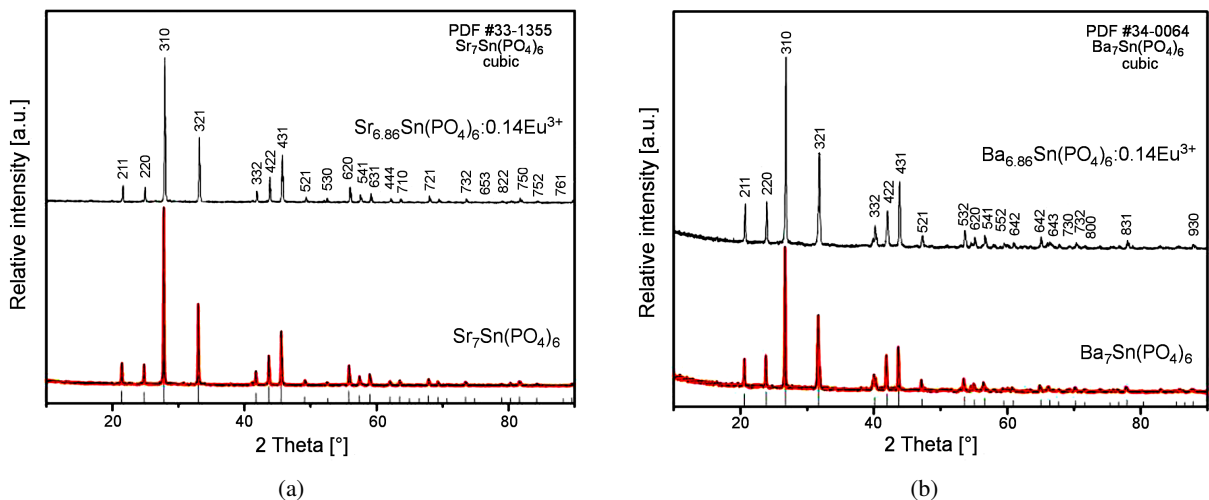


Figure 1. X-ray diffraction patterns of: a) $\text{Sr}_7\text{Sn}(\text{PO}_4)_6$ and $\text{Sr}_{6.86}\text{Sn}(\text{PO}_4)_6 : 0.14\text{Eu}^{3+}$ and b) $\text{Ba}_7\text{Sn}(\text{PO}_4)_6$ and $\text{Ba}_{6.86}\text{Sn}(\text{PO}_4)_6 : 0.14\text{Eu}^{3+}$

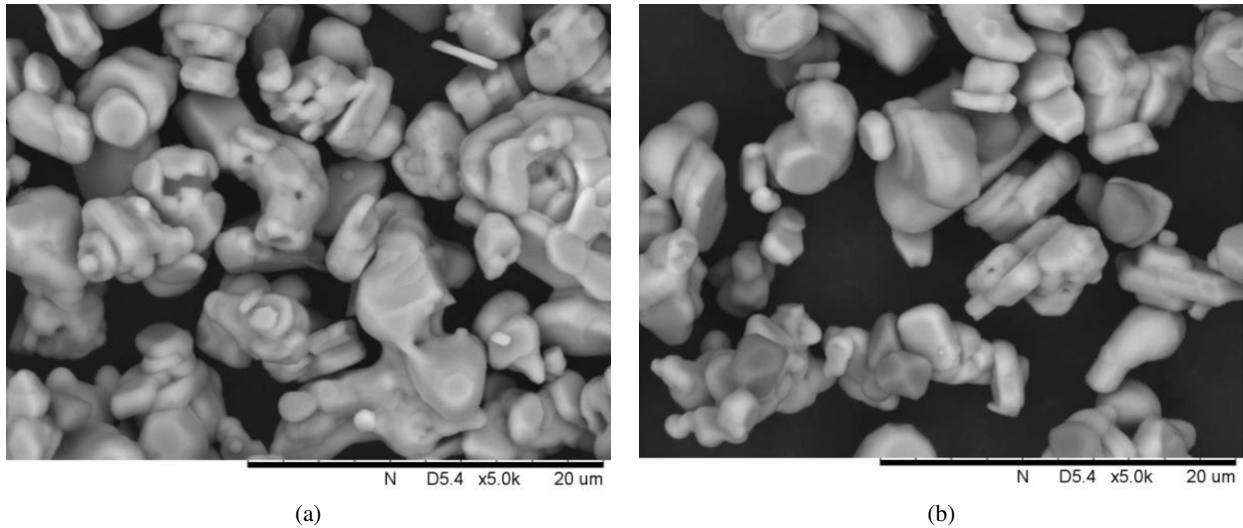


Figure 2. SEM images of: a) $\text{Sr}_{6.86}\text{Sn}(\text{PO}_4)_6:0.14\text{Eu}^{3+}$ and b) $\text{Ba}_{6.86}\text{Sn}(\text{PO}_4)_6:0.14\text{Eu}^{3+}$ phosphor

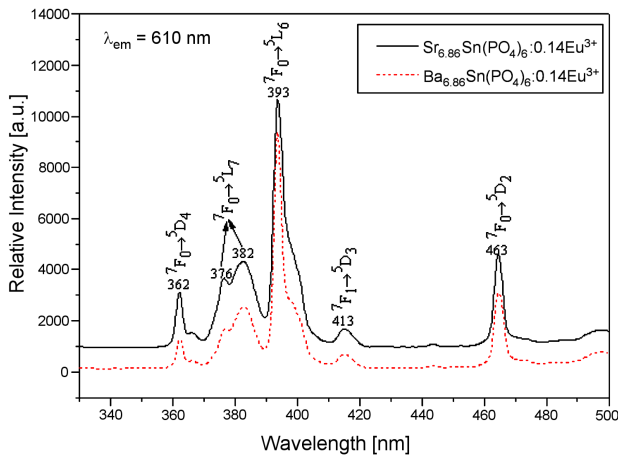


Figure 3. Excitation spectra of $\text{Sr}_{6.86}\text{Sn}(\text{PO}_4)_6:0.14\text{Eu}^{3+}$ and $\text{Ba}_{6.86}\text{Sn}(\text{PO}_4)_6:0.14\text{Eu}^{3+}$ samples

They exhibit similar excitation bands positions and relative intensities, indicating that excitation bands

stem from the same electronic state. The excitation bands located at 362 nm, 393 nm, 413 nm and 463 nm are attributed to the ${}^7\text{F}_0 \rightarrow {}^5\text{D}_1$, ${}^7\text{F}_0 \rightarrow {}^5\text{L}_6$, ${}^7\text{F}_1 \rightarrow {}^5\text{D}_3$ and ${}^7\text{F}_0 \rightarrow {}^5\text{D}_2$ transitions of Eu^{3+} , respectively, and the ${}^7\text{F}_0 \rightarrow {}^5\text{L}_7$ transition of Eu^{3+} splits into two bands located at 376 nm and 382 nm. These phosphors can be excited with wavelengths of 395 nm and 465 nm nicely in agreement with the widely applied near-UV LEDs and InGaN blue LED.

The emission spectra of the host $\text{M}_7\text{Sn}(\text{PO}_4)_6$ and doped $\text{M}_{6.86}\text{Sn}(\text{PO}_4)_6:0.14\text{Eu}^{3+}$ samples ($\text{M} = \text{Sr}, \text{Ba}$) were shown in Fig. 4. The emission spectra of the $\text{Sr}_{6.86}\text{Sn}(\text{PO}_4)_6:0.14\text{Eu}^{3+}$ phosphor under 395 nm and 465 nm excitation show roughly the same emission bands, except for the difference in intensity (Fig. 4a). The emission bands at about 591 nm, 610 nm and 647 nm are assigned to transitions of ${}^5\text{D}_0 \rightarrow {}^7\text{F}_J$ ($J = 1-3$), respectively. The emission bands at about 576 nm and 696 nm are supposed to be the host-related excitation, ascribing to the overlapping of the host (its emis-

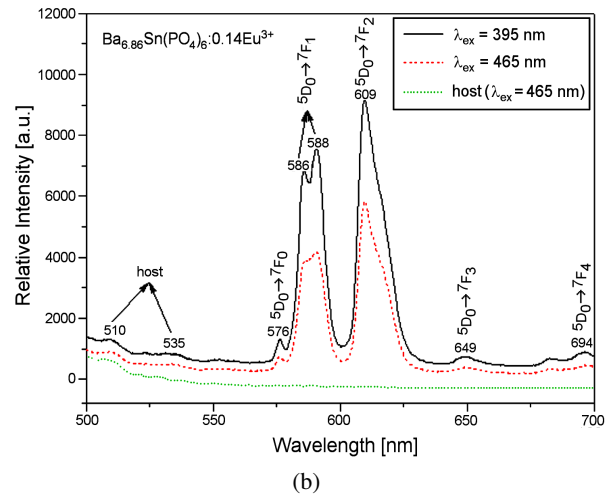
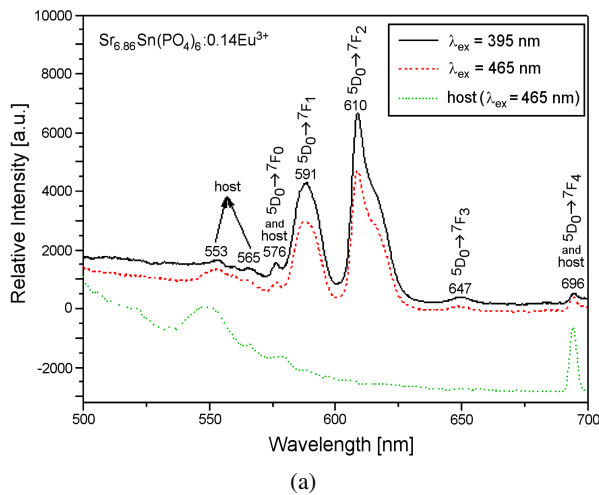


Figure 4. Emission spectra of: a) host $\text{Sr}_7\text{Sn}(\text{PO}_4)_6$ and doped $\text{Sr}_{6.86}\text{Sn}(\text{PO}_4)_6:0.14\text{Eu}^{3+}$ samples; and b) host $\text{Ba}_7\text{Sn}(\text{PO}_4)_6$ and doped $\text{Ba}_{6.86}\text{Sn}(\text{PO}_4)_6:0.14\text{Eu}^{3+}$ samples

sion spectrum is the yellow line in Fig. 4a) with ${}^5D_0 \rightarrow {}^7F_0$ and ${}^5D_0 \rightarrow {}^7F_4$, respectively. Apart from above obvious emission bands, the excitation spectra of the $\text{Sr}_{6.86}\text{Sn}(\text{PO}_4)_6:0.14\text{Eu}^{3+}$ phosphor contain two weak shoulder bands at about 553 nm and 565 nm, which is consistent with results of the excitation spectrum of the host $\text{Sr}_7\text{Sn}(\text{PO}_4)_6$.

As it can be seen from Fig. 4b, similar to the $\text{Sr}_{6.86}\text{Sn}(\text{PO}_4)_6:0.14\text{Eu}^{3+}$ phosphors, there is only a tiny distinction in intensity between the emission spectra of the $\text{Ba}_{6.86}\text{Sn}(\text{PO}_4)_6:0.14\text{Eu}^{3+}$ phosphors under 395 nm and 465 nm excitations. Nevertheless, the ${}^5D_0 \rightarrow {}^7F_J$ ($J = 0-4$) transition of Eu^{3+} emission bands exhibit slight blue-shifted emissions (relative to the corresponding emission bands in the emission spectra of the sample $\text{Sr}_{6.86}\text{Sn}(\text{PO}_4)_6:0.14\text{Eu}^{3+}$) located at 576 nm, 586 nm and 588 nm (split into two bands), 609 nm, 649 nm and 694 nm, respectively. It is because the electronegativity of Ba (0.89) is smaller than that of Sr (0.95), which makes the bonding strength between Ba^{2+} and negatively charged phosphate groups stronger than that of Sr^{2+} [12], leading to the energy transmission of the $\text{Ba}_7\text{Sn}(\text{PO}_4)_6$ host lattice (absorbing group $[\text{PO}_4]$) to the activation centre and the following electromagnetic radiation [13] is higher. This is also in accordance with the splitting comparison of $\text{Eu}^{3+} {}^5D_0 \rightarrow {}^7F_1$ transition in the samples $\text{Ba}_7\text{Sn}(\text{PO}_4)_6$ and $\text{Sr}_7\text{Sn}(\text{PO}_4)_6$. Definitely, the weak shoulder excitation bands below 560 nm originate from the host lattice excitation as it can be concluded from the comparison to the excitation spectrum of the host $\text{Ba}_7\text{Sn}(\text{PO}_4)_6$. The emission intensity corresponding to the 465 nm excitation is slightly lower than that of 395 nm because of the relatively lower absorption at this wavelength (Fig. 4). The appearance of the host lattice excitation bands in the excitation spectra of phosphors indicates that there exists efficient energy transfer from the host lattice of $\text{M}_7\text{Sn}(\text{PO}_4)_6$ ($\text{M} = \text{Sr}, \text{Ba}$) to Eu^{3+} ions.

It is well known that the efficient Eu^{3+} -activated

phosphors mainly depend on the absorption of the host and energy transfer efficiency [14]. It can be concluded from these results that PO_4^{3-} plays an important role in this novel phosphor. It absorbs the energy and then transfers it to Eu^{3+} , which increases the excited energy of Eu^{3+} and enhances the emission efficiency. Accordingly, the novel phosphor could be regarded as an efficient luminescent material.

The change of emission intensity and wavelength for the samples $\text{M}_7\text{Sn}(\text{PO}_4)_6:\text{Eu}^{3+}$ ($\text{M} = \text{Sr}, \text{Ba}$) as a function of Eu^{3+} concentration ($x = 0.005, 0.01, 0.015, 0.02, 0.02, 0.025, 0.03$ and 0.35) was shown in Fig. 5. For both investigated systems lower Eu^{3+} doping concentrations lead to weak luminescence, while higher doping beyond an optimum causes concentration quenching of the Eu^{3+} emission. The highest integrated emission intensity is noted at the Eu^{3+} concentration taken as the critical concentration. Generally, energy migration processes increase the probability that the optical excitation is trapping at defects or impurity sites, enhancing non-radiative relaxation. As the excitation energy migrates among a large number of centres before being emitted, the excitation energy may transfer between the close Eu^{3+} ions by the exchange interaction. With the increase in Eu^{3+} concentration, the average distance between Eu^{3+} ions decreases. This favours the energy transfer, and the critical concentration corresponds to the sufficient reduction in the average distance. Further reduction leads to cross relaxation namely above mentioned non-radiative relaxation, which causes concentration quenching. On the other hand, a decrease in the activator concentration decreases the energy stored by the ions. In the specific systems such as $\text{M}_7\text{Sn}(\text{PO}_4)_6:\text{Eu}^{3+}$ ($\text{M} = \text{Sr}, \text{Ba}$), the critical concentration of the activator (Eu^{3+}) was found to be 0.175 mol and 0.21 mol per formula unit for the $\text{Sr}_{7-x}\text{Sn}(\text{PO}_4)_6:x\text{Eu}^{3+}$ and $\text{Ba}_{7-x}\text{Sn}(\text{PO}_4)_6:x\text{Eu}^{3+}$, respectively. This result is mainly attributed to two reasons: i) the unit cell volume of $\text{Ba}_7\text{Sn}(\text{PO}_4)_6$ (12299 \AA^3) is

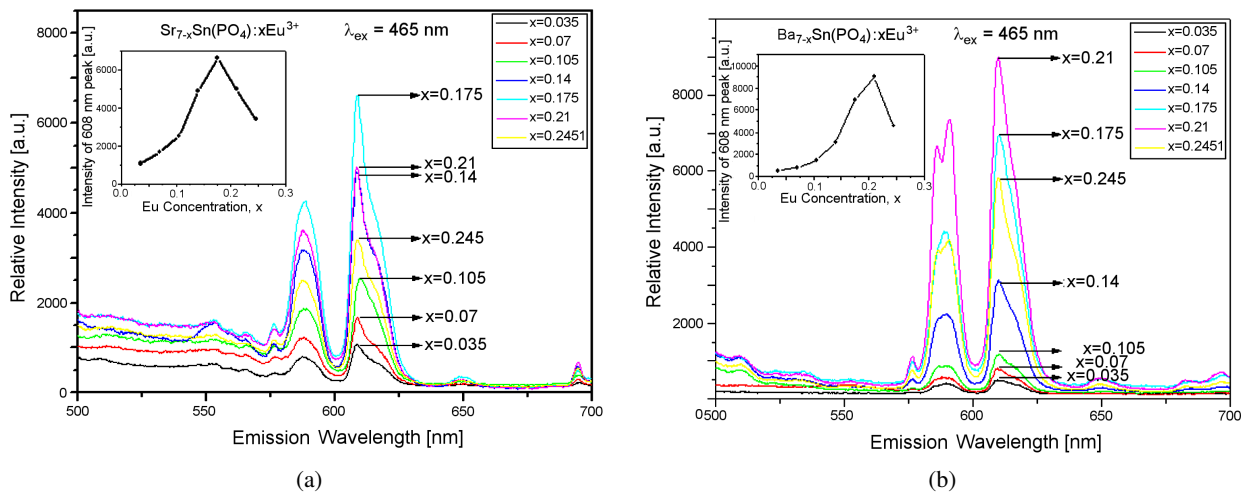


Figure 5. Emission spectra of: a) $\text{Sr}_{7-x}\text{Sn}(\text{PO}_4)_6:x\text{Eu}^{3+}$ and b) $\text{Ba}_{7-x}\text{Sn}(\text{PO}_4)_6:x\text{Eu}^{3+}$ (where $x = 0.035, 0.07, 0.105, 0.14, 0.175, 0.21, 0.245$)

much larger than that of $\text{Sr}_7\text{Sn}(\text{PO}_4)_6$ (10599 \AA^3), which causes increase in the critical concentration to achieve the best average distance of Eu^{3+} ions in two extremely similar cubic crystal structures; ii) the stronger interaction between activation centres with the host structure in $\text{Ba}_{7-x}\text{Sn}(\text{PO}_4)_6 : x\text{Eu}^{3+}$ weakens the energy migration and the cross relaxation between the activation centres.

IV. Conclusions

The novel red phosphors $\text{M}_{7-x}\text{Sn}(\text{PO}_4)_6 : x\text{Eu}^{3+}$ (where $\text{M} = \text{Sr}, \text{Ba}$ and $x = 0, 0.035, 0.07, 0.105, 0.14, 0.175, 0.21, 0.245$) were synthesized by the conventional solid-state reaction at $1200 \text{ }^\circ\text{C}$ for 2 h. The quenching concentration in the $\text{Ba}_7\text{Sn}(\text{PO}_4)_6$ is (0.21 mol per formula unit) higher than in the $\text{Sr}_7\text{Sn}(\text{PO}_4)_6$ (0.175 mol per formula unit) due to the relatively larger unit cell volume and crystal field effects of the $\text{Ba}_7\text{Sn}(\text{PO}_4)_6$. It is also discovered that PO_4^{3-} absorbs the energy and then transfers it to Eu^{3+} , which increases the excited energy of Eu^{3+} and enhances the emission efficiency. These phosphors can be efficiently excited by UV (395 nm) and visible blue (465 nm) light nicely matching the output wavelengths of the near-UV LEDs and InGaN blue LED chips and emits the red light. The $\text{M}_{7-x}\text{Sn}(\text{PO}_4)_6 : x\text{Eu}^{3+}$ ($\text{M} = \text{Sr}, \text{Ba}$) phosphor may be a good candidate for light-emitting diodes application.

Acknowledgement: This work was supported by the National Natural Science Foundation of China [grant numbers 51162013, 51362014]; the Major Discipline Academic and Technical Leader Training Plan Project of Jiangxi Province [grant number 20113BCB22009]; the Science and Technology Supporting Plan Project of Jiangxi Province, China [grant number 20111BBE50018]; the Youth Science Foundation of Jiangxi Province, China [grant number 20171BAB216009]; the Science Foundation of Jiangxi Provincial Department of Education, China [grant number GJJ150887]; the Youth Science Foundation of Jiangxi Provincial Department of Education, China [grant number GJJ150892]; the postdoctoral researchers preferred funded projects of Jiangxi Province [grant number 2013KY34]; and the Jingdezhen Science and technology program [grant number 20161GYZD011-007].

References

1. J. Kido, M. Kimura, K. Nagai, "Multilayer white light-emitting organic electroluminescent device", *Science*, **267** [5202] (1995) 1332.
2. S. Pimputkar, J.S. Speck, S.P. DenBaars, S. Nakamura, "Prospects for led lighting", *Nat. Photonics*, **3** [4] (2009) 180–182.
3. S. Neeraj, N. Kijima, A.K. Cheetham, "Novel red phosphors for solid-state lighting: the system $\text{NaM}(\text{WO}_4)_{2-x}(\text{MoO}_4)_x : \text{Eu}^{3+}$, ($\text{M} = \text{Gd}, \text{Y}, \text{Bi}$)", *Chem. Phys. Lett.*, **387** [1-3] (2004) 2–6.
4. G. Gundiah, Y. Shimomura, N. Kijim, A.K. Cheetham, "Novel red phosphors based on vanadate garnets for solid state lighting applications", *Chem. Phys. Lett.*, **455** [4] (2008) 279–283.
5. A. Potdevin, G. Chadeyron, R. Mahiou, "Tb³⁺-doped yttrium garnets: promising tunable green phosphors for solid-state lighting", *Chem. Phys. Lett.*, **490** [1] (2010) 50–53.
6. R.L. Toquin, A.K. Cheetham, "Red-emitting cerium-based phosphor materials for solid-state lighting applications", *Chem. Phys. Lett.*, **423** [4-6] (2006) 352–356.
7. J.S. Bae, K.S. Shim, B.K. Moon, "Enhanced luminescent characteristics of $\text{Y}_{2-x}\text{Gd}_x\text{O}_3 : \text{Eu}^{3+}$ ceramic phosphors by Li-doping", *J. Korean Phys. Soc.*, **46** [5] (2005) 1193–1197.
8. Z.W. Pei, Q. Su, S.H. Li, "Investigation on the luminescence properties of Dy^{3+} and Eu^{3+} in alkaline-earth borates", *J. Lumin.*, **50** [2] (1991) 123–126.
9. X.M. Liu, C.X. Li, Z.W. Quan, Z.Y. Cheng, J. Lin, "Tunable luminescence properties of $\text{CaIn}_2\text{O}_4 : \text{Eu}^{3+}$ phosphors", *J. Phys. Chem. C*, **111** [44] (2007) 16601–16607.
10. S.F. Wang, K.K. Rao, Y.R. Wang, Y.F. Hsu, S.H. Chen, Y.C. Lu, "Structural characterization and luminescent properties of a red phosphor series: $\text{Y}_{2-x}\text{Eu}_x(\text{MoO}_4)_3$, ($x = 0.4\text{--}2.0$)", *J. Am. Ceram. Soc.*, **92** [8] (2009) 1732–1738.
11. Y.R. Do, J.W. Bae, "Application of photoluminescence phosphors to a phosphor-liquid crystal display", *J. Appl. Phys.*, **88** [8] (2000) 4660–4665.
12. R.C. Ropp, *Luminescence and the Solid State*, Elsevier, Amsterdam, The Netherlands, 1991.
13. A. Nag, N. Kutty, "Role of interface states associated with transitional nanophase precipitates in the photoluminescence enhancement of $\text{SrTiO}_3 : \text{Pr}^{3+}, \text{Al}^{3+}$ ", *J. Mater. Chem.*, **13** [9] (2003) 2271–2278.
14. G. Blasse, "On the Eu^{3+} fluorescence of mixed metal oxides. IV. The photoluminescent efficiency of Eu^{3+} -activated oxides", *J. Chem. Phys.*, **45** [7] (1966) 2356–2360.